

# Chitosan-coated nanostructured lipid carriers of fenofibrate with enhanced oral bioavailability and efficacy

Yong-Chul Pyo, Phuong Tran, Dong-Hyun Kim, Jeong-Sook Park \*

Department of Physical Pharmacy, College of Pharmacy, Chungnam National University, Republic of Korea

## ARTICLE INFO

### Keywords:

fenofibrate  
hyperlipidemia  
chitosan  
nanostructured  
lipid  
carrier  
poorly soluble

## ABSTRACT

Fenofibrate is frequently used to lower cholesterol levels in cardiovascular disease. Owing to its poor solubility and high gastrointestinal permeability, it is classified as a Biopharmaceutics Classification System class II compound. The aim of this study was to improve the solubility and bioavailability of fenofibrate by formulating it as fenofibrate-loaded nanostructured lipid carriers (FFB-NLCs) and coating it with a biodegradable polymer to allow controlled drug release. Chitosan-coated nanostructured lipid carriers (CF-NLCs) were prepared via an ultrasonication method using chitosan as the biodegradable polymer, stearic acid as the solid lipid, oleic acid as the liquid lipid, and Tween 80 as the surfactant. To study encapsulation efficiency and solubility conditions, stearic acid/oleic acid ratios were varied as 80/20, 70/30, 60/40, and 50/50 (mg/mg), by adjusting chitosan ratio. Chitosan is an adhesive polymer, coating the surface of the NLC to improve its bioavailability. All NLC formulations demonstrated a particle size of approximately 200 nm and a polydispersity index below 0.3. The encapsulation efficiencies of the NLC formulations were above 85%. For CF-NLCs, the solubility and encapsulation efficiency of fenofibrate were increased when compared with those of a commercial fenofibrate formulation. The pharmacokinetic and pharmacodynamic parameters of fenofibrate in the form of CF-NLCs were improved after oral administration. CF-NLCs can be used for allowing controlled release and improving the bioavailability and stability of fenofibrate.

## 1. Introduction

Recently discovered novel drug candidates are insoluble in the aqueous phase [1]. Despite their excellent efficacy, some candidates are limited in therapeutic use owing to their poor aqueous solubility [2]. Novel concepts are crucial to address this shortcoming. One strategy is to develop a carrier that can be encapsulated, protected, and released under specific and desired conditions [3]. As guest molecules electrostatically enter the hydrophobic matrix, lipid materials are suitable candidates for the formulation of active hydrophobic delivery systems. Furthermore, various techniques, additives, and formulations are required to enhance the solubility of poorly soluble drugs. Self-emulsifying drug delivery systems (SEDDS) [4], self-microemulsifying drug delivery systems (SMEDDS) [5–7], amorphous solid dispersions [8], nanosuspensions [9], and liquid crystals [10,11] have been tested. Several lipid-based carriers have been established including emulsions, liposomes, solid lipid nanoparticles (SLNs), as well as the more recently developed, nanostructured lipid carriers (NLCs).

Fenofibrate, a biopharmaceutical classification system class II drug, is used to treat hypercholesterolemia and hypertriglyceridemia [8]. Fenofibrate is marketed globally and has been well-described pharmacologically [12]. The drug is poorly water-soluble, partly owing to its high hydrophobicity ( $\log P = 5.24$ , Fig. S1). Therefore, it exhibits poor oral bioavailability. For poorly water-soluble drugs, the rate of absorption depends on the rate of dissolution, which in turn determines the bioavailability [13]. Lipidil® Supra, a brand name for fenofibrate, has been used commercially for the treatment of hyperlipidemia (Green Cross Co., Ltd., Seoul, Korea), and is consumed orally once a day.

It is challenging to administer lipid-based drug carriers as enzymatic hydrolysis by lipase causes rapid elimination of particles, resulting in the loss of a certain amount of bioactive molecules. Hence, these particles should be protected from gastrointestinal environment. Polymer coating and encapsulation of nanoparticles in polymeric microparticles (synthetic and natural polymers) have been used to protect the formulation from enzymatic attack. A polymer coating system with natural polymers (e.g., hyaluronic acid and chitosan) improves the oral bioavailability of bioactive molecules [14]. This strategy was applied to develop NLCs

\* Corresponding author.

E-mail address: [eicos@cnu.ac.kr](mailto:eicos@cnu.ac.kr) (J.-S. Park).

<https://doi.org/10.1016/j.colsurfb.2020.111331>

Received 5 December 2019; Received in revised form 10 August 2020; Accepted 14 August 2020

Available online 26 August 2020

0927-7765/© 2020 Elsevier B.V. All rights reserved.

with improved mucoadhesive properties and sustained release profiles.

NLCs are prepared by a composite of different lipid molecules, for example solid lipids are mixed with liquid lipids. When liquid lipids are added, the formation of complete lipid crystals is distorted, increasing the loading capacity, reducing the particle size, increasing the degree of gelation, and increasing drug disappearance following storage. Additionally, NLCs can induce the drug to enter the lymphatic pathway or Payer's patches, which is well known for promoting oral absorption of drugs [15].

The aim of this study was to prepare fenofibrate-loaded NLCs using a biodegradable polymer coating to enhance solubility and bioavailability. In addition, the lipid-reducing effect of the formulation by increased bioavailability was confirmed. The most useful lipids and excipients were selected to optimize the solubility of fenofibrate. CF-NLC formulations were prepared using the hot high-shear homogenizer and ultrasonicator technique. Physicochemical characterization was performed by assessing the particle size, zeta potential, encapsulation efficiency, differential scanning calorimetry (DSC), powder X-ray diffraction (PXRD), and scanning electron microscopy (SEM). Additionally, pharmacokinetic and pharmacodynamic studies in rats were performed to confirm the significant increase in the plasma concentration of fenofibrate and therapeutic effect of CF-NLC and FFB-NLC formulations when it compared with raw fenofibrate and commercially available Lipidil® Supra.

## 2. Materials and Methods

### 2.1. Materials

Fenofibrate, chitosan, Tween 80, Tween 20, sodium tripolyphosphate (TPP), and phosphatidyl choline were purchased from Sigma-Aldrich (St. Louis, MO, USA). Stearic acid, oleic acid, palmitic acid, beeswax, myristic acid, lauric acid, coconut oil, olive oil, linseed oil, labrasol, cotton oil, and castor oil were purchased from Samchun Chemicals (Seoul, Korea). The commercial fenofibrate product purchased was Lipidil® Supra (Green Cross Co., Ltd, Seoul, Korea). Cholesterol fluorometric and triglyceride colorimetric assay kits were purchased from Cayman Chemicals (Ann Arbor, MI, USA). Acetonitrile and methanol for high-performance liquid chromatography (HPLC) were purchased from Samchun Pure Chemicals Co., Ltd. (Seoul, Korea). Fetal bovine serum, antibiotics, and Dulbecco's modified Eagle medium (DMEM) were procured from Hyclone™ (Logan, UT, USA). All other chemicals were of analytical grade, used without further purification.

### 2.2. Screening of solid lipids, liquid lipids, and surfactants

Fenofibrate is a poorly soluble drug in the aqueous phase. Hence, NLCs should be optimized to improve the solubility of fenofibrate. A solubility test for fenofibrate in various lipids and surfactants, was conducted to optimize the formulation. The solid lipids were heated to a temperature of 10°C above melting point. An excess amount of fenofibrate was added to the lipids and surfactants. Solid lipids were supplemented with fenofibrate until the lipids were opaque. Liquid lipids and surfactants containing excess fenofibrate were centrifuged and diluted for sampling. The clear supernatants were analyzed by HPLC (Shimadzu, Kyoto, Japan) [16,17]. To assess the solubility in lipids and surfactants, the concentration of fenofibrate was determined using HPLC (Shimadzu). The flow rate of the mobile phase of acetonitrile : water (7.5:2.5, v/v) was 1 mL/min. A Capcell Pak C18 column (150 mm × 4.6 mm internal diameter, 5-µm diameter particles; Shiseido, Osaka, Japan) was used for the separation. After filtering, 20 µL of the sample was injected into the HPLC system equipped with ultraviolet detection at 280 nm.

### 2.3. Preparation of fenofibrate-loaded NLCs (FFB-NLCs) and chitosan-coated NLCs (CF-NLCs)

FFB-NLCs were prepared using a hot high shear homogenizer and an ultrasonicator. For the NLCs, stearic acid and oleic acid, selected by the previous screening test, were mixed at various ratios (7:3, 6:4, 5:5, 4:6, and 3:7; the total amount of lipids was 600 mg) with fenofibrate and 30 mg of phosphatidyl choline in methanol at a high temperature (Table S1). Following the heating and mixing process, 10 mL of 2% Tween 80 solution was added to the lipids and the mixed solution was sonicated to form FFB-NLCs using an ultrasonicator. The sample temperature was maintained at approximately 60 °C during the sonication procedure. Finally, the hot sonicated solution was cooled slowly to 20 °C for stabilization and stored at 4 °C. All formulations were designed to contain 4.5 mg/mL FFB.

To prepare chitosan-coated FFB-NLCs (C-NLCs), the prepared FFB-NLCs were coated with chitosan. Chitosan was dissolved in acetic acid (0.06% v/v), and the prepared chitosan solution (0.15% w/v) was stabilized under stirring for 24 h. TPP solution (0.05% w/v) was prepared by dissolving TPP in distilled water, and chitosan and TPP solutions were filtered using a 0.45 µm filter membrane. The pH of the chitosan and TPP solutions was adjusted to 4 and 7, respectively, using 0.1 M sodium hydroxide solution and 0.1 M HCl. FFB-NLCs were added to the chitosan solution (ratio of FFB solution/chitosan solution = 1/10). The TPP solution was added dropwise to the CF-NLC dispersion (ratio of CF-NLCs/TPP = 3/1) under magnetic stirring (550 rpm). The solution was maintained at room temperature to establish crosslinking. CF-NLCs were centrifuged at 2000 ×g for 15 min at 4°C and washed three times with distilled water to remove excess TPP [14]. The resultant particles were dried on aluminum trays in the dark for 24 h.

### 2.4. Characterization of the prepared CF-NLCs

The particle size of the formulation and polydispersity index (PDI) were determined using a Zetasizer Nano S90 (Malvern Instruments, Malvern, UK). The surface charge was determined by measuring the zeta potential using Zetasizer nano-Z (Malvern Instruments) [18]. The prepared formulations were diluted in a 1:10 ratio with distilled water. All measurements were performed in triplicate.

To determine the encapsulation efficiency, 1.5 mL of the NLC formulation was taken in Eppendorf tubes and centrifuged at 10,000 ×g for 15 min. After the free drug was separated from the NLC formulation by centrifugation, the supernatant was collected and analyzed using the HPLC method previously described. The amount of the unencapsulated drug in the aqueous medium was measured, and the encapsulation efficiency was calculated.

To evaluate the stability of NLCs in gastric fluid, the particle size, PDI, and zeta potential were determined after suspending (1:10) in a pH 1.2 buffer. All measurements were performed in triplicate.

### 2.5. Differential scanning calorimetry (DSC)

The prepared formulation, drug, and excipients were analyzed by DSC (Mettler-Toledo, Columbus, OH, USA). The samples were lyophilized using a freeze dryer (FDU-1200, EYELA, Tokyo, Japan) and 2 mg samples were placed on aluminum pans for the DSC analysis. The samples were heated from 25 °C to 200 °C, at a rate of 5 °C/min.

### 2.6. Powder X-ray diffraction (PXRD)

The PXRD study was conducted using a powder X-ray diffractometer (D/MAX-2200 Ultima, Rigaku International Corporation, Tokyo, Japan). The samples were exposed to nickel-filtered CuKα radiation (40 kV, 40 mA). The samples used for PXRD analysis were FFB-NLCs and CF-NLCs. All samples were lyophilized powder using a freeze dryer (FDU-1200, EYELA).

## 2.7. Scanning electron microscopy (SEM)

The morphology of fenofibrate, FFB-NLCs, and CF-NLCs was studied using SEM (S-4800, Hitachi, Tokyo, Japan). To obtain solid samples for SEM, the FFB-NLC and CF-NLC formulations were lyophilized using a freeze dryer (FDU-1200, EYELA). Fenofibrate, FFB-NLC, and CF-NLC powders were placed on a carbon tape was coated with platinum for 90 s under vacuum. The samples were visualized under an acceleration voltage of 5.0 kV.

## 2.8. In vitro release study

The in vitro release studies were conducted using the dialysis technique to evaluate the fenofibrate release profile from each formulation. A dialysis membrane (Spectrum Chemical, New Brunswick, NJ, USA) with a molecular weight cutoff of 100 kDa was used. A phosphate buffer (pH 7.4) containing 0.3% sodium lauryl sulfate was used as the receptor medium (500 mL) at 37 °C and 75 rpm [18,19]. The in vitro release of fenofibrate from the optimized CF-NLC formulation (F2) was compared with the release of the pure drug and the uncoated FFB-NLCs. The formulations (equivalent to 100 mg of fenofibrate) were placed in the donor compartment. The solution in the receptor side was maintained at 37 ± 0.5 °C. The samples were withdrawn at 5, 10, 15, 30, 45, 60, 90, 120, 180, 240, and 300 min, and replaced with an equal volume of freshly prepared PBS (pH 7.4) [20]. The samples were analyzed using HPLC (Shimadzu) at 280 nm.

## 2.9. Cell viability

The MTT assay was used to evaluate cell viability. Madin-Darby Canine Kidney (MDCK) cells were seeded in a 96-well plate (Nunc, Thermo Fisher, Rochester, NY, USA) in DMEM (50,000 cells/well). After 24 h of seeding, the medium in each well was replaced with the test drugs (various concentrations of raw fenofibrate, FFB-NLCs, and CF-NLCs in DMEM). The plate was incubated for 24 and 48 h. Next, the wells were emptied and filled with 100 µL of 3-(4,5-dimethylthiazol-2-yl)-2,5-diphenyl tetrazolium bromide solution dissolved in DMEM (5 mg/mL). After 4 h, MTT solution was removed and each well was refilled with 200 µL/well of dimethylsulfoxide (DMSO). Subsequently, the absorbance of the solution was measured using a microplate reader (Infinite M200 PRO; Tecan Trading AG, Männedorf, Switzerland) at 570 nm (Table S2) [21]. The spectrophotometer was calibrated to zero absorbance using medium without cells. Cell viability (%) relative to control, containing the cell culture medium without sample, was calculated as  $[A]_{\text{test}} \times 100 / [A]_{\text{control}}$ .

## 2.10. Stability test of FFB-NLCs and CF-NLCs

Particle size, zeta potential, and encapsulation efficiency were evaluated. The optimized NLC formulations were stored at 4 °C for 60 days. Physical stability was determined on the day of production, and after 30 and 60 days of storage [8].

## 2.11. Pharmacokinetic study

For the pharmacokinetic study, male Sprague-Dawley (SD) rats, weighing 220–250 g (aged 8 weeks), were obtained from Samtako (Osan, Korea). All animal experiments were performed after receiving approval from the Ethics Committee of Chungnam National University (no. 201903A-CNU-36). During the experiment, three animals were housed per cage under appropriate conditions; 22 ± 2 °C, 50–60% relative humidity, under a 12-h light/dark cycle. The rats were randomly divided into four groups (n = 3). After fasting the rats for 12 h, each rat was administered a single oral dose of raw fenofibrate, FFB-NLCs, commercial product (Lipidil® Supra), and CF-NLCs, at 100 mg/kg of FFB. After drug administration, 0.4 mL of blood was drawn from

the retro-orbital plexus into heparinized polyethylene tubes at predetermined time intervals of 20, 40, 60, 90, 120, 240, 480, 720, and 1440 min [22,23]. The blood samples were immediately centrifuged at 10,000 ×g for 10 min and maintained in the deep freezer at –70 °C before analysis. The collected plasma samples were analyzed using HPLC to quantify the content of fenofibric acid. Before analysis, the plasma samples (100 µL) were deproteinated by the addition of 100 µL of a 1:1 mixture of acetonitrile and 70% perchloric acid and vortex mixing for 1 min. The Eppendorf tubes were centrifuged at 10,000 ×g for 10 min at approximately 4 °C. The collected supernatant was then filtered through a 0.45 µm syringe filter and directly injected into the HPLC system (Shimadzu). Clofibrac acid was used as internal standard. A Capcell Pak C18 column (Shiseido) was used for the separation. Optimum separation was performed with 55:45:0.2 (v/v, %) acetonitrile : distilled water : acetic acid. The signals were monitored using a UV detector at a wavelength of 287 nm. The column temperature was set at 30 °C, and the flow rate was at 1 mL/min. For recording and calculations, the LabSolution software (Kyoto, Japan) was used. The pharmacokinetic parameters including area under the plasma concentration–time curve up to time infinity ( $AUC_{0 \rightarrow \infty}$ ), peak plasma concentration ( $C_{\text{max}}$ ), time to reach peak plasma concentration ( $T_{\text{max}}$ ), mean residence time, and terminal half-life ( $t_{1/2}$ ) were determined using the WinNonlin™ software (Version 5.2, Scientific Consulting Inc., Apex, NC, USA) by performing non-compartmental analysis.

## 2.12. Pharmacodynamics study

Male SD rats (weighing 220–250 g) were used to evaluate drug efficacy in acute hyperlipidemia-induced rats (n = 3). The poloxamer-induced rat hyperlipidemia model was used to evaluate the anti-hyperlipidemic activity of the fenofibrate formulations. For inducing acute hyperlipidemia, poloxamer 407 was used. The rats were fasted for 12 h before hyperlipidemia induction, and were randomly divided into six groups (n = 4): (i) normal group (injected normal saline instead of poloxamer, receiving no treatment), (ii) control group (subjected to poloxamer induction, receiving no treatment), (iii) raw suspension group (subjected to poloxamer induction, treated with raw fenofibrate suspension), (iv) FFB-NLCs group (subjected to poloxamer induction, treated with FFB-NLCs), and (v) Lipidil® Supra group (subjected to poloxamer induction, treated with Lipidil® Supra), (vi) CF-NLCs group (subjected to poloxamer induction, treated with CF-NLCs). In all groups, except the normal group, poloxamer 407, dissolved in 0.9% normal saline, was intraperitoneally injected to rats at a dose of 400 mg/kg [24, 25]. The use of poloxamer 407 was considered a more suitable alternative to Triton for increasing hepatic triglyceride production rates [26]. After the dosing and treatment of the animals, blood samples were collected at 0, 24, 36, and 48 h. Here, 0 h implied a time point before the induction of acute hyperlipidemia. Blood (1 mL) was withdrawn from the retro-orbital plexus of the rats into heparinized tubes and centrifuged at 10,000 ×g for 10 min at 4 °C to separate the plasma. Cholesterol fluorometric and triglyceride colorimetric assay kits were used to assay serum cholesterol and triglycerides, respectively [27].

## 2.13. Statistical analysis

Statistical analysis was performed with Student's *t*-test using SigmaPlot (ver. 12.5; SYSTAT, Inc., Chicago, IL, USA). The data are expressed as mean ± standard deviation. For all analyses,  $P < 0.05$  (\*) and  $P < 0.1$  (\*\*) were considered statistically significant.

## 3. Results and Discussion

### 3.1. Solubility test

The solubility of fenofibrate in various materials is shown in Fig. 1. The solubility of fenofibrate was analyzed using HPLC (Shimadzu) [19].

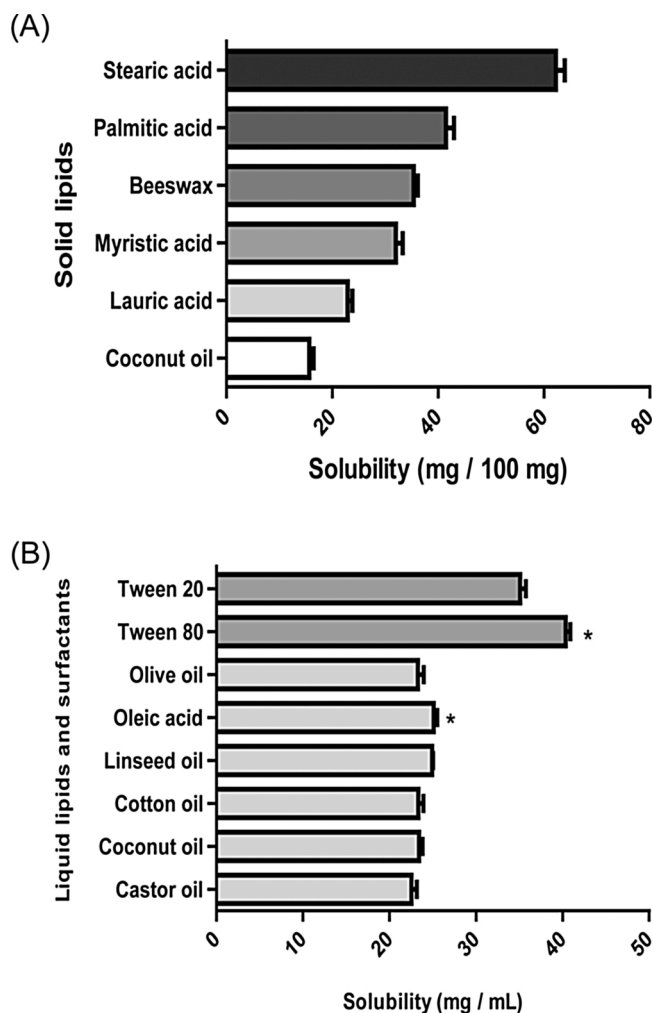


Fig. 1. Fenofibrate solubility. Screening of (A) solid lipids and (B) liquid materials. Each point represents the mean  $\pm$  S.D. ( $n = 3$ ). In all analyses, comparison between Tween 80 and Tween 20, oleic acid and olive oil;  $P < 0.1$  (\*).

Among the solid lipids, liquid lipids, and surfactants, the highest solubility of fenofibrate was demonstrated in stearic acid ( $60.27 \pm 0.93$  mg/100 mg), followed by Tween 80 ( $39.33 \pm 0.59$  mg/mL) and oleic acid ( $25.33 \pm 0.75$  mg/mL). Furthermore, the solubility of fenofibrate in stearic acid was 2-fold higher than that in myristic acid. Therefore, stearic acid, oleic acid, Tween 80, and phosphatidyl choline were chosen for the formulation.

### 3.2. Optimization of the component ratio of CF-NLC formulation

The effect of the oleic acid-to-stearic acid ratio was evaluated for further optimization of the formulation (Table S1). As the concentration of oleic acid affects the viscosity of FFB-NLCs, various formulations were prepared using a constant portion of Tween 80 (2% w/w) and various stearic acid-to-oleic acid ratios (30, 40, 50, 60, and 70 wt% of stearic

acid/total lipid), and were designated as F1, F2, F3, F4, and F5, respectively. Formulation F5 could not be prepared as the stearic acid content was lower than that present in other formulations. Therefore, it was not included in further studies as the NLC forms were not maintained.

### 3.3. Characterization of CF-NLCs and FFB-NLCs formulations

The particle size, zeta potential, encapsulation efficiency, and loading capacity of CF-NLCs and FFB-NLCs formulations are shown in Table 1. The particle sizes of F1, F2, F3, and F4 ( $1125.2 \pm 14.2$  nm,  $1085.9 \pm 14.8$  nm,  $1058.5 \pm 15.2$  nm, and  $1155.4 \pm 15.4$  nm, respectively), were increased by chitosan coating when compared with those of FFB-NLCs. PDI values were similar between CF-NLCs and FFB-NLCs. The zeta potential of CF-NLCs demonstrated a positive charge value. When CS was added to prepare F1, F2, F3, and F4 formulations, the zeta potential of NLC formulations was increased from  $-28.1$  mV (FFB-NLCs) to  $22.4$  mV (F1),  $25.4$  mV (F2),  $21.7$  mV (F3), and  $22.0$  mV (F4), respectively (Table 1). This was similar to the tendency observed in a previous NLC study [28].

In NLCs, the encapsulation efficiency of fenofibrate was determined as a critical factor for optimizing the formulations. Furthermore, the encapsulation efficiency was similar among formulation groups; the encapsulation efficiency of F1, F2, F3, F4, and FFB-NLCs was  $88.0 \pm 1.3\%$ ,  $87.6 \pm 2.1\%$ ,  $85.4 \pm 1.6\%$ ,  $84.2 \pm 1.4\%$ , and  $86.5 \pm 2.4\%$ , respectively. Fenofibrate is highly lipophilic ( $\log P > 5$ ) and can be easily incorporated into the lipid matrix. Tran et al. have reported that loading efficiencies greater than 9% were obtained using different compositions of NLCs with Compritol and Labrafil [29]. Lower loading efficiencies of CF-NLCs and FFB-NLCs could be attributed to the different composition of our formulations, including stearic acid, oleic acid, and phosphatidyl choline. In the experimental group, F2 was the most optimized formulation, and hence referred to as CF-NLCs.

As the stability of NLCs in the gastric fluid is an important parameter, the particle size, PDI, and zeta potential were determined in a pH 1.2 buffer. The particle sizes of FFB-NLCs and F2 were  $314.2 \pm 16.8$  nm and  $1289.3 \pm 88.6$  nm, respectively. After suspension in a pH 1.2 buffer, PDI values were similar between FFB-NLCs and CF-NLCs. However, the zeta potential of FFB-NLCs and CF-NLCs was slightly altered to  $-3.2 \pm 1.8$  mV and  $14.4 \pm 0.4$  mV, respectively. Therefore, these findings suggest that FFB-NLCs and CF-NLCs might be stable in gastric fluid, and CF-NLCs would exhibit enhanced oral bioavailability.

### 3.4. DSC analysis

DSC is widely used to determine the thermal transition of polymeric materials used for formulation preparation and to assess the crystalline state of drugs and carriers in formulations. DSC thermograms of raw fenofibrate, stearic acid, chitosan, physical mixture, FFB-NLCs, and CF-NLCs were recorded (Fig. 2A). The thermogram of raw fenofibrate showed a sharp single melting peak at approximately  $77.9^\circ\text{C}$ , corresponding to the melting point of the crystalline drug. The thermograms of stearic acid and the physical mixture showed a similar sharp single melting peak at  $62.2^\circ\text{C}$ ; however, chitosan showed no melting peak. FFB-NLCs showed melting peaks at  $62.2^\circ\text{C}$ , and  $165^\circ\text{C}$ , while CF-NLCs

Table 1  
Physicochemical properties of CF-NLCs (mean  $\pm$  SD,  $n = 3$ )

Formulation	Particle size (nm)	Polydispersity index	Zeta potential (mV)	Encapsulation efficiency (%)	Loading capacity (%)
F1	$1125.2 \pm 14.2$	$0.235 \pm 0.02$	$22.4 \pm 1.7$	$88.0 \pm 1.3$	$5.8 \pm 0.2$
F2	$1085.9 \pm 14.8$	$0.195 \pm 0.01$	$25.4 \pm 1.4$	$87.6 \pm 2.1$	$5.7 \pm 0.2$
F3	$1058.5 \pm 15.2$	$0.215 \pm 0.01$	$21.7 \pm 2.5$	$85.4 \pm 1.6$	$5.6 \pm 0.1$
F4	$1155.4 \pm 15.4$	$0.208 \pm 0.01$	$22.0 \pm 1.2$	$84.2 \pm 1.4$	$5.5 \pm 0.1$
FFB-NLCs	$278.5 \pm 18.2$	$0.380 \pm 0.01$	$-28.1 \pm 1.5$	$86.5 \pm 2.4$	$5.7 \pm 0.2$

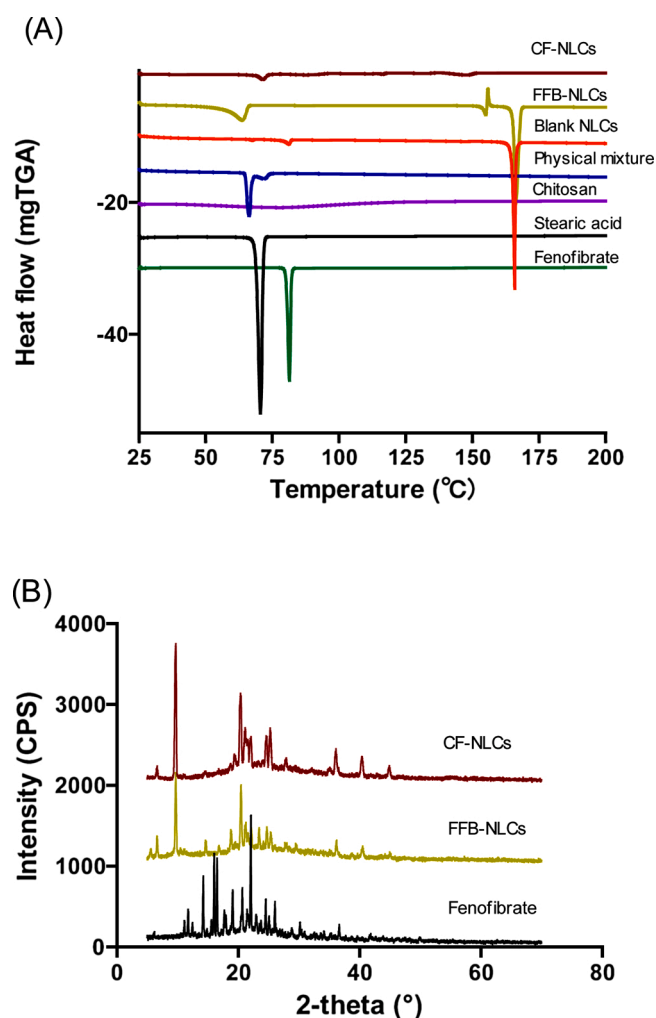


Fig. 2. (A) DSC thermograms of raw fenofibrate powder, stearic acid, chitosan, physical mixture, FFB-NLCs and CF-NLCs and (B) PXRD of FFB-NLCs and CF-NLCs.

showed no melting peaks [29,30]. This was attributed to the conversion of raw fenofibrate to the amorphous form rather than the crystalline form in the CF-NLC formulation, and the conversion was influenced by chitosan.

### 3.5. PXRD analysis

PXRD diffractograms are shown in Fig. 2B. The diffractogram of raw fenofibrate indicated sharp characteristic peaks at diffraction angles (2 Theta) of 11.8°, 14.3°, 16.1°, 16.6°, and 22.2°. These peaks correspond to the known crystalline fenofibrate peak reported in the literature. Moreover, these peaks were not observed in the FFB-NLC formulations [30]. These findings indicated that CF-NLCs were formulated well using the coating method.

### 3.6. SEM

The morphology of raw fenofibrate, FFB-NLCs, and CF-NLCs was observed by SEM. The SEM images of raw fenofibrate, FFB-NLCs, and CF-NLCs are shown in Fig. 3A. The surface of crystalline raw fenofibrate was sharper than that of FFB-NLC and CF-NLC formulations. The surface of raw fenofibrate was irregularly shaped, demonstrating an irregular model of the crystalline form with various particle sizes. In contrast, the surface of CF-NLCs was smoother and circular, and the particle size was larger than that of FFB-NLCs, appearing to be connected to each

formulation [31]. This may be related to the presence of chitosan on the particle surface. Notably, the surface of FFB-NLCs was regularly shaped.

### 3.7. In vitro release study

The in vitro release test was performed for 5 h. The amount of FFB released from the NLC dispersion was determined by the in vitro dialysis bag technique. The in vitro release of CF-NLCs showed burst release in the first 30 min, and complete release was observed at 5 h (Fig. 3B). The in vitro drug release studies demonstrated that approximately 92% of the drug was released at the end of 5 h for CF-NLCs, with 91% release observed from FFB-NLCs, and only 28% of the drug released from pure fenofibrate at the end of 5 h. The increased dissolution rate of CF-NLCs could be mainly attributed to the obvious liquefaction of the drug in the lipid solvents. Both formulations, CF-NLCs and FFB-NLCs, demonstrated similar dissolution patterns. Similar results have been reported in previous investigations [20,32]. In the case of CF-NLCs, the drug was present in lipids with the polymer, thereby showing sustained drug release.

### 3.8. Cell viability

MDCK cells were used for the evaluation of cellular toxicity. The concentration range of fenofibrate was 100–1000 µg/mL, the equivalent in vivo concentration range. This study was used to evaluate cell viability after growing at the various concentrations of different formulations [34]. As shown in Table S2, at 200 µg/mL, the cell viability with every sample was as high as 90%. This implied that the ingredients used for the formulating the NLCs were non-toxic at this concentration. However, at higher concentrations, cell viability decreased regardless of the formulation [35]. As cell viability did not vary significantly based on the formulation and the cell viability was high, it was concluded that these preparations demonstrated no toxicity toward MDCK cells at experimental concentrations.

### 3.9. Stability

The stability of NLC formulations was determined by monitoring the particle size, PDI, zeta potential, and encapsulation efficiency under storage at 4 °C (Table S3). The initial particle sizes of FFB-NLCs and CF-NLCs were  $278.5 \pm 18.2$  nm and  $1085.9 \pm 14.8$  nm, respectively, which were altered to  $385.4 \pm 24.9$  nm and  $920.9 \pm 27.8$  nm, respectively, after 60 days of storage at 4 °C. The PDI values of FFB-NLCs and CF-NLCs were modified from 0.380 and 0.195 to 0.316 and 0.239, respectively, whereas the corresponding zeta potentials were altered from -28.1 mV and 25.4 mV to -27.8 mV and 22.8 mV, respectively. The encapsulation efficiency values of FFB-NLCs and CF-NLCs decreased from 86.5% and 87.6% to 66.1% and 81.9%, respectively. Accordingly, CF-NLC can be considered more stable than FFB-NLC as the encapsulation efficiency of CF-NLC was reduced to a lesser extent than that of FFB-NLC. Hence, the encapsulated drug could be leaked from the uncoated NLCs. Simultaneously, it was suggested that the encapsulation efficiency of CF-NLCs was not significantly decreased as the chitosan coating could prevent leakage of encapsulated drug from the CF-NLCs. Similarly, hydrophobic drug in aqueous dispersions was stabilized in cationic lipid bilayer fragments and surrounding the assembly with a biocompatible biopolymer such as carboxymethylcellulose [35].

### 3.10. Pharmacokinetic study

The pharmacokinetic study investigated four formulations: raw fenofibrate, Lipidil® Supra, FFB-NLCs, and CF-NLCs. The mean plasma concentration versus time profiles of fenofibric acid are shown in Fig. 4. The pharmacokinetic parameters are summarized in Table 2. The AUC values of raw fenofibrate, FFB-NLCs, Lipidil® Supra, and CF-NLCs were  $68.9 \pm 2.9$  h·µg/mL,  $227.6 \pm 7.2$  h·µg/mL,  $357.5 \pm 12.2$  h·µg/mL, and  $416.9 \pm 2.6$  h·µg/mL, respectively. Meanwhile, the  $C_{max}$  values of raw

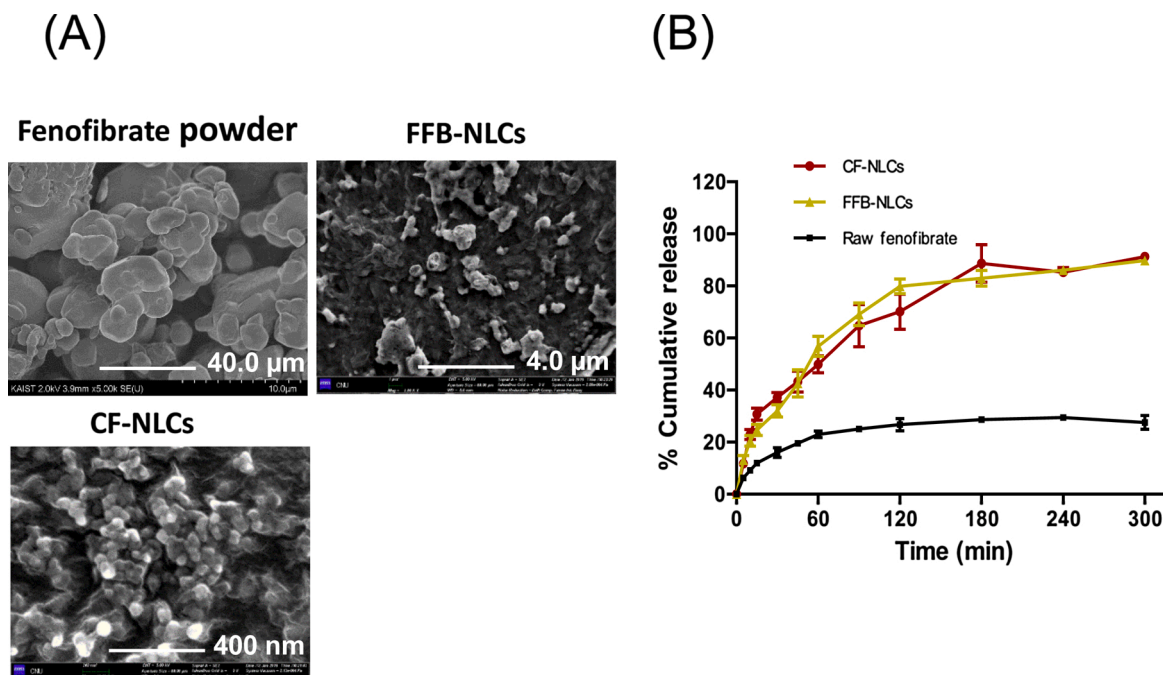


Fig. 3. (A) Scanning electron microscopy (SEM) images of fenofibrate powder, FFB-NLCs, and CF-NLCs after lyophilization. (B) In vitro release profiles of raw fenofibrate, FFB-NLCs, and CF-NLCs in pH 7.4 phosphate buffer containing 0.3% sodium lauryl sulfate (SLS). Each point represents the mean ± S.D. (n = 3).

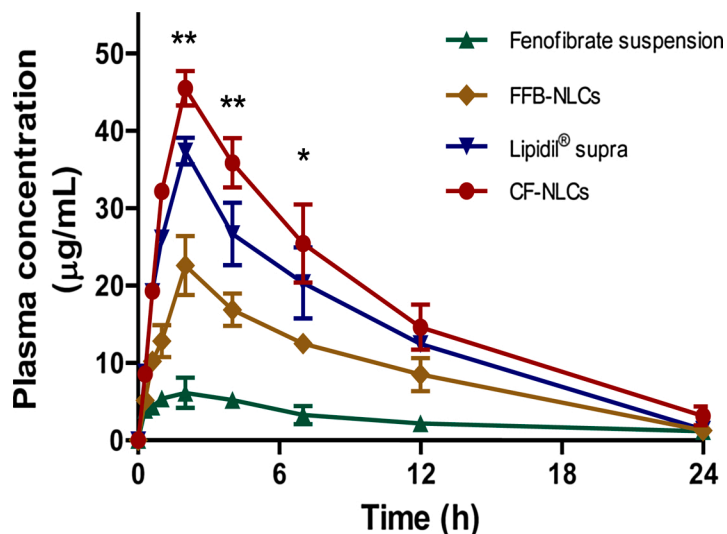


Fig. 4. Plasma concentration-time profiles of fenofibric acid after oral administration of raw fenofibrate, FFB-NLCs, CF-NLCs formulations, and the commercial product (Lipidil® supra). Each dose was equivalent to 100 mg/kg bodyweight fenofibrate. Each point represents the mean ± S.D. (n = 3). In all analyses, comparison between CF-NLCs and Lipidil® Supra;  $P < 0.05$  (\*\*) and  $P < 0.1$  (\*).

Table 2

Non-compartmental pharmacokinetic parameters after oral administration of fenofibrate formulations and chitosan-coated fenofibrate nanostructured lipid carriers (CF-NLC) (equivalent to 100 mg/kg of fenofibrate (FFB)) to rats (mean ± SD, n = 3)

Parameter	Raw FFB	FFB-NLCs	Lipidil® Supra	CF-NLCs
AUC <sub>0-∞</sub> (μg h/mL)	68.9 ± 2.9	227.6 ± 7.2	357.5 ± 12.2	416.9 ± 2.6*
AUMC <sub>0-∞</sub> (μg h <sup>2</sup> /mL)	1167.8 ± 76.6	2000.56 ± 55.8	2774.6 ± 62.9	3290.0 ± 314.2*
MRT (h)	13.7 ± 0.6	8.5 ± 0.1	7.6 ± 0.1	7.6 ± 0.6
C <sub>max</sub> (μg/mL)	6.1 ± 0.1	23.9 ± 1.5	37.3 ± 1.7	46.7 ± 1.9*
t <sub>1/2</sub> lambda z (h)	9.3 ± 0.3	4.0 ± 0.2	4.7 ± 0.03	4.6 ± 0.9
T <sub>max</sub> (h)	2.17 ± 0.6	1.93 ± 0.3	1.96 ± 0.3	2.11 ± 0.3

In all analyses, comparison between CF-NLCs and Lipidil® Supra;  $P < 0.1$  (\*).

fenofibrate, FFB-NLCs, Lipidil® Supra, and CF-NLCs were  $6.1 \pm 0.1 \mu\text{g}/\text{mL}$ ,  $23.9 \pm 1.5 \mu\text{g}/\text{mL}$ ,  $37.3 \pm 1.7 \mu\text{g}/\text{mL}$ , and  $46.7 \pm 1.9 \mu\text{g}/\text{mL}$ , respectively. In the CF-NLC groups, the  $\text{AUC}_{0-12\text{h}}$  (6-fold) and  $\text{C}_{\text{max}}$  (7.8-fold) were significantly higher than those observed in the raw fenofibrate group ( $P < 0.005$ ). Even when compared with the FFB-NLC group, the CF-NLC group showed higher  $\text{AUC}_{0-12\text{h}}$  (1.8-fold) and  $\text{C}_{\text{max}}$  (1.9-fold) values ( $P < 0.05$ ). Interestingly, the AUC and  $\text{C}_{\text{max}}$  values of Lipidil® Supra and CF-NLCs differed significantly despite the similarity in distribution rates [8,36].

To improve the oral bioavailability of FFB, several approaches have been investigated including nanocrystals, SMEDDS, nanosuspension, solid dispersion, and SLNs [8,13,20,22,23]. Among these strategies, SLNs have several advantages; they are physically stable, protect the incorporated sensitive drug molecules from degradation, and lower blood circulation time. Based on these advantages, SLNs have been developed into NLCs, as second generation SLNs, with a solid matrix blended with a liquid lipid (oil) to form an unstructured matrix; NLCs exhibit enhanced drug loading capacity and reduced drug expulsion from the matrix during storage [29,33]. In general, the small particle size of NLCs might lead to have exhibited enhanced adhesion to the gastrointestinal wall or entry into the intervillar spaces and prolonged interaction time with the gastrointestinal tract, enhancing drug bioavailability [29]. The use of chitosan to prepare oral nanoparticle drug carriers improves absorption and stability in the gastrointestinal tract [37]. In this study, FFB-NLCs were coated with chitosan to obtain CF-NLCs to make the NLCs mucoadhesive. The CF-NLCs demonstrated 2-fold higher drug absorption than FFB-NLCs ( $P < 0.05$ ), despite the absorption rate constant ( $K_a$ ) of CF-NLCs, FFB-NLCs and Lipidil® Supra. The bioavailability of vitamin B12 is reportedly increased by chitosan without affecting its absorption rate constant [37]. Table 2 shows that the chitosan coating improved the half-life,  $\text{C}_{\text{max}}$ , and  $\text{AUC}_{0-\infty}$  of fenofibrate when compared with Lipidil® Supra ( $P < 0.1$ ). The significant increase in the bioavailability of repaglinide could be attributed to the mucoadhesive properties of chitosan, which interacts with the negatively charged mucosal membranes and acts as a permeation enhancer by opening tight junctions [38,39].

The  $\text{AUC}_{0-12\text{h}}$  and  $\text{C}_{\text{max}}$  values of CF-NLCs were 1.16-fold and 1.25-fold higher than those of the commercial product, respectively. This indicates that the increase in drug solubility by formulating it as NLCs and coating with a biodegradable polymer can increase dissolution rate and permeability, thereby improving bioavailability and therapeutic effects. As is known, fenofibrate is almost completely metabolized to fenofibric acid after entering the body; therefore, the concentration of fenofibric acid indicates the amount of absorbed fenofibrate. The concentration of fenofibrate in the blood increased steadily after drug administration, and the plasma concentration peaked at 2 h. Similar pharmacokinetic data for fenofibrate have been reported, but the plasma concentration of fenofibric acid in our study was higher than that reported previously [8].

### 3.11. Pharmacodynamics study

A model of acute hyperlipidemia, which can be used to evaluate the lipid-lowering abilities of a drug was established by using poloxamer [24,25]. Poloxamer 407 is a nonionic surfactant known to increase the total cholesterol and triglyceride levels in the blood by inhibiting the lipoclastic enzyme that eliminates lipids in the body [24,25]. After the intraperitoneal administration of poloxamer 407, it was confirmed that the increase in the blood lipid levels were confirmed. After injection of poloxamer 407, raw fenofibrate, FFB-NLCs, Lipidil® Supra, and CF-NLCs were administered, the rats were divided to six groups; drug-free, control and each formulation. After collecting the blood sample at 12, 24, 36, and 48 h, the total cholesterol and triglyceride levels in the blood of rats are shown in Fig. 5 and Table S4. Lipid levels increased in all groups after poloxamer injection at 0 h. However, after 24, 36, and 48 h, lipase activity was reduced, and the total cholesterol and triglyceride levels

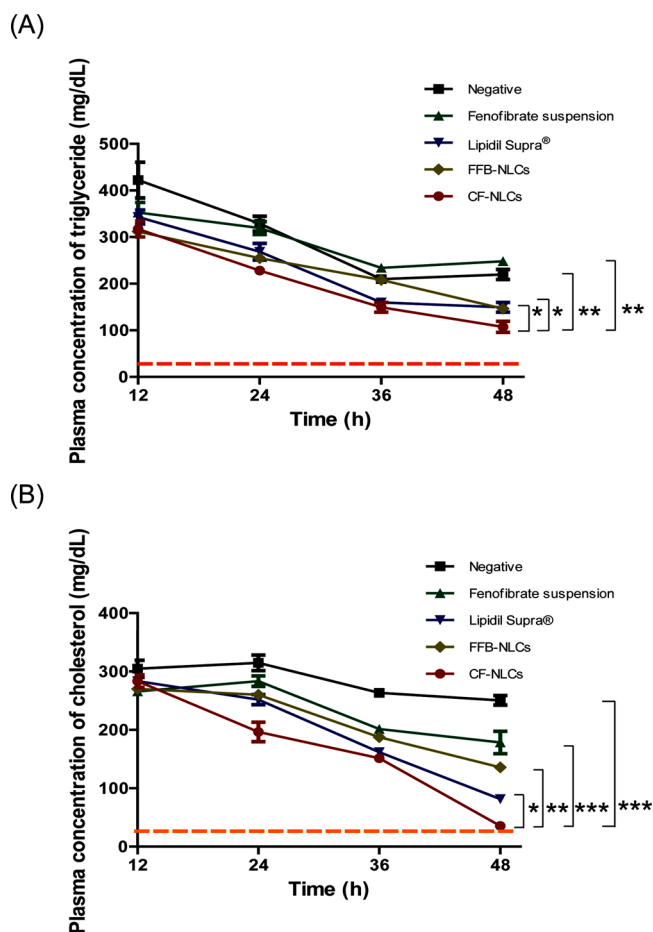


Fig. 5. Plasma concentrations of (A) cholesterol and (B) triglyceride after intraperitoneal injection of poloxamer 407. The dotted line is each normal value of plasma concentration. Each point represents the mean  $\pm$  S.D. ( $n = 4$ ). In all analyses, comparison between CF-NLCs and Lipidil® Supra;  $P < 0.005$  (\*\*\*),  $P < 0.05$  (\*\*), and  $P < 0.1$  (\*).

decreased in line with the therapeutic effect of fenofibrate. In the control group, there was no significant difference in lipid levels between 0 and 48 h. In contrast, the groups injected with poloxamer 407 increased their blood cholesterol to demonstrate a value of  $304.6 \pm 28.8 \text{ mg}/\text{dL}$  at 12 h [25]. Cholesterol levels at 36 h after the administration of raw fenofibrate, FFB-NLCs, Lipidil® Supra, and CF-NLCs were  $178.4 \pm 38.3 \text{ mg}/\text{dL}$ ,  $135.9 \pm 12.3 \text{ mg}/\text{dL}$ ,  $81.6 \pm 4.9 \text{ mg}/\text{dL}$ , and  $35.5 \pm 5.3 \text{ mg}/\text{dL}$ , respectively. Simultaneously, the concentration of triglycerides increased to  $422.3 \pm 76.4 \text{ mg}/\text{dL}$  at 12 h after the poloxamer 407 injection [25]. Triglyceride levels after the administration of raw fenofibrate, FFB-NLCs, Lipidil® Supra, and CF-NLCs at 36 h were  $248.2 \pm 16.9 \text{ mg}/\text{dL}$ ,  $146.5 \pm 7.2 \text{ mg}/\text{dL}$ ,  $149.3 \pm 20.9 \text{ mg}/\text{dL}$ , and  $107.5 \pm 23.5 \text{ mg}/\text{dL}$ , respectively. Based on these results, it can be observed that CF-NLCs and Lipidil® Supra reduce lipid levels to a greater extent than raw fenofibrate. These results are in good agreement with pharmacokinetic results, demonstrating the improved bioavailability of FFB-NLCs and CF-NLCs. Moreover, the CF-NLCs group showed a 5-fold and 2.3-fold lower total cholesterol and triglyceride levels than the raw fenofibrate group, respectively. This is the high degree of lipid reduction compared with any formulation [40]. After 48 h, the degree of lipid reduction did not differ from that observed at 12 h (Table S4). Notably, FFB-NLCs, Lipidil® Supra, and CF-NLCs demonstrated better lipid-lowering effects than raw fenofibrate. Particularly, CF-NLCs restored the lipid levels to levels observed in the normal control group after 48 h. These results suggest that the NLC formulation and chitosan coating increased the solubility and permeability of fenofibrate.

#### 4. Conclusion

In this study, fenofibrate was formulated into a lipid-based drug delivery system and coated with a biodegradable polymer. The interactions between NLCs and positively charged chitosan allowed the formation of nanoparticles of controlled size and resulted in a gel in the presence of TPP. The zeta potential, DSC, and PXRD data showed that the NLC formulation was successfully coated with chitosan. This resulted in increased concentrations of fenofibrate in the rat plasma and an increased lipid-lowering effect. The formulation was stable for 8 weeks. Thus, the water solubility and bioavailability of fenofibrate can be improved by formulating it as CF-NLCs.

#### CRedit authorship contribution statement

**Yong-Chul Pyo:** Conceptualization, Methodology, Formal analysis, Investigation, Writing - original draft, Writing - review & editing. **Puong Tran:** Methodology, Investigation, Writing - review & editing. **Dong-Hyun Kim:** Methodology. **Jeong-Sook Park:** Conceptualization, Writing - original draft, Writing - review & editing, Project administration.

#### Declaration of Competing Interest

The authors declare that they have no known competing financial interests or personal relationships that could have appeared to influence the work reported in this paper.

#### Acknowledgement

This work was supported by the National Research Foundation of Korea (NRF) grant funded by the Korea government (MSIT) (NRF-2019R1H1A2039708 and NRF-2020R1F1A1075127).

#### Appendix A. Supplementary data

Supplementary material related to this article can be found, in the online version, at doi:<https://doi.org/10.1016/j.colsurfb.2020.111331>.

#### References

- [1] Y. Kawabata, K. Wada, M. Nakatani, S. Yamada, S. Onoue, Formulation design for poorly water-soluble drugs based on biopharmaceutics classification system: Basic approaches and practical applications, *Int. J. Pharm.* 420 (2011) 1–10, <https://doi.org/10.1016/j.ijpharm.2011.08.032>.
- [2] W. Mehnert, K. Mäder, Solid lipid nanoparticles: production, characterization and applications, *Adv. Drug Deliv. Rev.* 64 (2012) 83–101.
- [3] D.J. McClements, Nanoparticle- and microparticle-based delivery systems: Encapsulation, protection and release of active compounds, CRC press (2014).
- [4] C. Menzel, T. Holzhausen, F. Laffleur, S. Zaichik, M. Abdulkarim, M. Gumbleton, A. Bernkop-Schnürch, In vivo evaluation of an oral self-emulsifying drug delivery system (SEDDS) for exenatide, *J. Control. Release* 277 (2018) 165–172.
- [5] R. Verma, V. Mittal, D. Kaushik, Quality based design approach for improving oral bioavailability of valsartan loaded SMEDDS and study of impact of lipolysis on the drug diffusion, *Drug Deliv. Lett.* 8 (2018) 130–139.
- [6] S. Dokania, A.K. Joshi, Self-microemulsifying drug delivery system (SMEDDS)–challenges and road ahead, *Drug Deliv.* 22 (2015) 675–690.
- [7] S.C. Patil, A.A. Tagalpalawar, C.R. Kokare, Natural anti-proliferative agent loaded self-microemulsifying nanoparticles for potential therapy in oral squamous carcinoma, *J. Pharm. Investig.* 49 (2019) 527–541.
- [8] J.B. Ahn, D.-H. Kim, S.-E. Lee, Y.-C. Pyo, J.-S. Park, Improvement of the dissolution rate and bioavailability of fenofibrate by the supercritical anti-solvent process, *Int. J. Pharm.* 564 (2019) 263–272, <https://doi.org/10.1016/j.ijpharm.2019.04.051>.
- [9] B.K. Ahuja, S.K. Jena, S.K. Paidi, S. Bagri, S. Suresh, Formulation, optimization and in vitro–in vivo evaluation of febuxostat nanosuspension, *Int. J. Pharm.* 478 (2015) 540–552.
- [10] S. Pisano, M. Giustiniani, L. Francis, D. Gonzalez, L. Margarit, I.M. Sheldon, D. Paolino, M. Fresta, R.S. Conlan, G.D. Healey, Liquid crystal delivery of ciprofloxacin to treat infections of the female reproductive tract, *Biomed. Microdevices* 21 (2019) 36.
- [11] R. Rajabalaya, M.N. Musa, N. Kifli, S.R. David, Oral and transdermal drug delivery systems: role of lipid-based lyotropic liquid crystals, *Drug Des. Devel. Ther.* 11 (2017) 393.
- [12] H. Murakami, R. Murakami, F. Kambe, X. Cao, R. Takahashi, T. Asai, T. Hirai, Y. Numaguchi, K. Okumura, H. Seo, Fenofibrate activates AMPK and increases eNOS phosphorylation in HUVEC, *Biochem. Biophys. Res. Commun.* 341 (2006) 973–978.
- [13] A.M. Yousef, D.W. Kim, Y.-K. Oh, C.S. Yong, J.O. Kim, H.-G. Choi, Enhanced oral bioavailability of fenofibrate using polymeric nanoparticulated systems: physicochemical characterization and in vivo investigation, *Int. J. Nanomedicine* 10 (2015) 1819.
- [14] H.H. Ali, F. Michaux, A.N. Khanji, J. Jasniewski, M. Linder, Chitosan-Shea butter solid nanoparticles assemblies for the preparation of a novel nanoparticles in microparticles system containing curcumin, *Colloids Surfaces A Physicochem, Eng. Asp.* 553 (2018) 359–367.
- [15] L. Montenegro, F. Lai, A. Offerta, M.G. Sarpietro, L. Micicche, A.M. Maccioni, D. Valenti, A.M. Fadda, From nanoemulsions to nanostructured lipid carriers: A relevant development in dermal delivery of drugs and cosmetics, *J. Drug Deliv. Sci. Technol.* 32 (2016) 100–112.
- [16] V. Makwana, R. Jain, K. Patel, M. Nivsarkar, A. Joshi, Solid lipid nanoparticles (SLN) of Efavirenz as lymph targeting drug delivery system: Elucidation of mechanism of uptake using chylomicron flow blocking approach, *Int. J. Pharm.* 495 (2015) 439–446.
- [17] M. Joshi, V. Patravale, Nanostructured lipid carrier (NLC) based gel of celecoxib, *Int. J. Pharm.* 346 (2008) 124–132.
- [18] W. Zhang, J. Liu, Q. Zhang, X. Li, S. Yu, X. Yang, J. Kong, W. Pan, Enhanced cellular uptake and anti-proliferating effect of chitosan hydrochlorides modified genistein loaded NLC on human lens epithelial cells, *Int. J. Pharm.* 471 (2014) 118–126.
- [19] G. Zoubari, S. Staufienbiel, P. Volz, U. Alexiev, R. Bodmeier, Effect of drug solubility and lipid carrier on drug release from lipid nanoparticles for dermal delivery, *Eur. J. Pharm. Biopharm.* 110 (2017) 39–46.
- [20] H. Patil, X. Feng, X. Ye, S. Majumdar, M.A. Repka, Continuous production of fenofibrate solid lipid nanoparticles by hot-melt extrusion technology: a systematic study based on a quality by design approach, *AAPS J.* 17 (2015) 194–205.
- [21] M. Pinheiro, R. Ribeiro, A. Vieira, F. Andrade, S. Reis, Design of a nanostructured lipid carrier intended to improve the treatment of tuberculosis, *Drug Des. Devel. Ther.* 10 (2016) 2467.
- [22] Y.-D. Cho, Y.-J. Park, In vitro and in vivo evaluation of a self-microemulsifying drug delivery system for the poorly soluble drug fenofibrate, *Arch. Pharm. Res.* 37 (2014) 193–203.
- [23] G. Quan, Q. Wu, X. Zhang, Z. Zhan, C. Zhou, B. Chen, Z. Zhang, G. Li, X. Pan, C. Wu, Enhancing in vitro dissolution and in vivo bioavailability of fenofibrate by solid self-emulsifying matrix combined with SBA-15 mesoporous silica, *Colloids Surfaces B Biointerfaces* 141 (2016) 476–482.
- [24] W.K. Palmer, E.E. Emeson, T.P. Johnston, Poloxamer 407-induced atherosclerosis in the C57BL/6 mouse, *Atherosclerosis* 136 (1998) 115–123.
- [25] N.Y. Yoon, H.R. Kim, H.Y. Chung, J.S. Choi, Anti-hyperlipidemic effect of an edible brown algae, *Ecklonia stolonifera*, and its constituents on poloxamer 407-induced hyperlipidemic and cholesterol-fed rats, *Arch. Pharm. Res.* 31 (2008) 1564–1571.
- [26] J.S. Millar, D.A. Cromley, M.G. McCoy, D.J. Rader, J.T. Billheimer, Determining hepatic triglyceride production in mice: comparison of poloxamer 407 with Triton WR-1339, *J. Lipid Res.* 46 (2005) 2023–2028.
- [27] T.J. Cole, M.C. Bellizzi, K.M. Flegal, W.H. Dietz, Establishing a standard definition for child overweight and obesity worldwide: international survey, *Bmj.* 320 (2000) 1240.
- [28] F.-Q. Hu, S.-P. Jiang, Y.-Z. Du, H. Yuan, Y.-Q. Ye, S. Zeng, Preparation and characterization of stearic acid nanostructured lipid carriers by solvent diffusion method in an aqueous system, *Colloids Surfaces B Biointerfaces* 45 (2005) 167–173.
- [29] R. Nair, A.C.K. Kumar, V.K. Priya, C.M. Yadav, P.Y. Raju, Formulation and evaluation of chitosan solid lipid nanoparticles of carbamazepine, *Lipids Health Dis.* 11 (2012) 72.
- [30] P. Ramalingam, Y.T. Ko, Enhanced oral delivery of curcumin from N-trimethyl chitosan surface-modified solid lipid nanoparticles: pharmacokinetic and brain distribution evaluations, *Pharm. Res.* 32 (2015) 389–402.
- [31] C.-Y. Zhuang, N. Li, M. Wang, X.-N. Zhang, W.-S. Pan, J.-J. Peng, Y.-S. Pan, X. Tang, Preparation and characterization of vinpocetine loaded nanostructured lipid carriers (NLC) for improved oral bioavailability, *Int. J. Pharm.* 394 (2010) 179–185.
- [32] D. Xia, N. Shrestha, J. van de Streek, H. Mu, M. Yang, Spray drying of fenofibrate loaded nanostructured lipid carriers, *Asian J. Pharm. Sci.* 11 (2016) 507–515.
- [33] Q. Liu, J. Li, G. Pu, F. Zhang, H. Liu, Y. Zhang, Co-delivery of baicalin and doxorubicin by hyaluronic acid decorated nanostructured lipid carriers for breast cancer therapy, *Drug Deliv.* 23 (2016) 1364–1368.
- [34] R. Kumar, A. Singh, K. Sharma, D. Dhasmana, N. Garg, P.F. Siril, Preparation, characterization and in vitro cytotoxicity of Fenofibrate and Nabumetone loaded solid lipid nanoparticles, *Mater. Sci. Eng. C* 106 (2020), 110184.
- [35] E.G. Lima, L.R. Gomes, A.M. Carmona-Ribeiro, Stable indomethacin dispersions in water from drug, ethanol, cationic lipid and carboxymethyl-cellulose, *Pharm. Nanotechnol.* 4 (2016) 126–135, <https://doi.org/10.2174/2211738504666160304195436>.
- [36] B. Bahloul, F. Safta, M.A. Lassoued, H. Dhotel, J. Seguin, N. Mignet, S. Sfar, Use of mouse model in pharmacokinetic studies of poorly water soluble drugs: application to fenofibrate, *J. Drug Deliv. Sci. Technol.* 43 (2018) 149–153.
- [37] Y. Goto, A. Masuda, T. Aiba, In vivo application of chitosan to improve bioavailability of cyanocobalamin, a form of vitamin B12, following intraintestinal administration in rats, *Int. J. Pharm.* 483 (2015) 250–255, <https://doi.org/10.1016/j.ijpharm.2015.02.016>.

- [38] Z. Karami, M.R. Saghatchi Zanjani, N. Nasihatsheno, M. Hamidi, Improved oral bioavailability of repaglinide, a typical BCS Class II drug, with a chitosan-coated nanoemulsion, *J. Biomed. Mater. Res. Part B Appl. Biomater.* 108 (2020) 717–728, <https://doi.org/10.1002/jbm.b.34426>.
- [39] M. Wang, M. Liu, T. Xie, B.-F. Zhang, X.-L. Gao, Chitosan-modified cholesterol-free liposomes for improving the oral bioavailability of progesterone, *Colloids Surfaces B Biointerfaces.* 159 (2017) 580–585, <https://doi.org/10.1016/j.colsurfb.2017.08.028>.
- [40] R.W. Mahley, T.P. Bersot, Drug therapy for hypercholesterolemia and dyslipidemia, *Goodman Gilman's Pharmacol, Basis Ther.* 11 (2001) 933.